Physics Letters B 695 (2011) 105–109

Contents lists available at ScienceDirect

Physics Letters B

www.elsevier.com/locate/physletb

Insights into the mechanisms and time-scales of breakup of ^{6,7}Li

D.H. Luong [a,*], M. Dasgupta [a], D.J. Hinde [a], R. du Rietz [a], R. Rafiei [a], C.J. Lin [a], M. Evers [a], A. Diaz-Torres [a,b]

[a] Department of Nuclear Physics, Research School of Physics and Engineering, The Australian National University, Canberra, ACT 0200, Australia
[b] Department of Physics, University of Surrey, Guildford, GU2 7XH, UK

ARTICLE INFO

Article history:
Received 16 July 2010
Received in revised form 26 October 2010
Accepted 5 November 2010
Available online 11 November 2010
Editor: V. Metag

Keywords:
Exclusive breakup
Transfer-breakup
Weakly-bound nuclei
Nuclear clusters
Fusion

ABSTRACT

Using a back-angle detector array covering 117° to 167°, coincidence measurements of breakup fragments at sub-barrier energies have enabled the complete characterisation of the breakup processes in the reactions of ^{6,7}Li with ^{208}Pb. Those breakup processes fast enough ($\sim 10^{-22}$ s) to affect fusion are identified through the measured relative energy of the two breakup fragments. The majority of these prompt breakup events are triggered by transfer of a neutron from ^{6}Li, and of a proton to ^{7}Li. These mechanisms, rather than breakup following direct projectile excitation, should thus be responsible for the majority of the ~30% suppression of complete fusion observed at above-barrier energies. Breakup characteristics thus depend both on the properties of the initial nucleus *and* its neighbours. Quantitative modelling of this two-step process will require development of a complete reactions model, relevant for reactions involving both α-cluster nuclei, and exotic nuclei near the neutron and proton drip-lines.

1. Introduction

The stability of both the helium atom and its nucleus (the α-particle) results from the filling of the lowest energy quantum state by a pair of electrons, or pairs of protons and neutrons respectively. This stability can cause nuclei to behave as though they *contain* α-particles. This is seen in α-decay of heavy nuclei, and in α-cluster structure in light nuclei. The clustering of neutrons and protons in nuclei, often in the form of α-particles, has a long and fascinating history. Well before the discovery of the neutron, Rutherford in 1921 pictured the nitrogen nucleus as composed of three α-particles and a proton [1]. Since then, α-clustering has remained a consistent feature of models of the structure of light nuclei, arising spontaneously from many different theoretical approaches [2]. In ^{12}C, the celebrated 3-α cluster excited state (the Hoyle state [3]) is critical to the synthesis of heavier elements in the Universe [4]. The lighter elements Li and Be show α-cluster structure in their ground-states [5,6], associated with low energy thresholds against cluster breakup. Breakup can occur in nuclear collisions if a state above the relevant breakup energy threshold is populated. This can happen by Coulomb or nuclear excitation of the projectile nucleus itself, or by a transfer reaction populating an unbound state in the projectile-like nucleus. Independent of the mechanism populating the unbound state, its cluster decay is called breakup [7–13]. Observations of ~30% suppression of complete fusion cross sections in reactions of Li and Be [14–18] were associated with their low breakup threshold energies. For ^{9}Be, measurements of sub-barrier breakup fragments [19] indicated a link between fusion suppression and *prompt* breakup (before reaching the fusion barrier), which reduces the flux of intact projectile nuclei available to participate in fusion. The capture of only one breakup fragment by the target, called incomplete fusion (ICF), was also observed [14,15].

It is clear that for a complete understanding of the effect of weak binding on fusion, it is critical to experimentally make the distinction between *prompt* breakup occurring on short time-scales ($\sim 10^{-22}$ s) and *delayed* breakup that occurs on longer time-scales. Experimental studies have so far been unable to unambiguously obtain this information. Furthermore, current quantum models of nuclear reactions are of limited use as they cannot separate complete and incomplete fusion, thus cannot model the effect of breakup on complete fusion [20,21]. For these experimental and theoretical reasons, a quantitative understanding of breakup and the suppression of complete fusion has not yet been attained. Thus, outcomes of reactions with weakly-bound nuclei from new radioactive ion beam accelerators cannot yet be predicted. This work aims to provide a complete picture of breakup in reactions of weakly-bound ^{6,7}Li nuclei, and to identify experimentally those breakup processes fast enough to affect fusion.

2. Experimental details and results

To experimentally identify and characterise all breakup mechanisms, it is necessary to simultaneously measure both breakup

* Corresponding author.
E-mail address: huy.luong@anu.edu.au (D.H. Luong).

0370-2693/$ – see front matter
doi:10.1016/j.physletb.2010.11.007

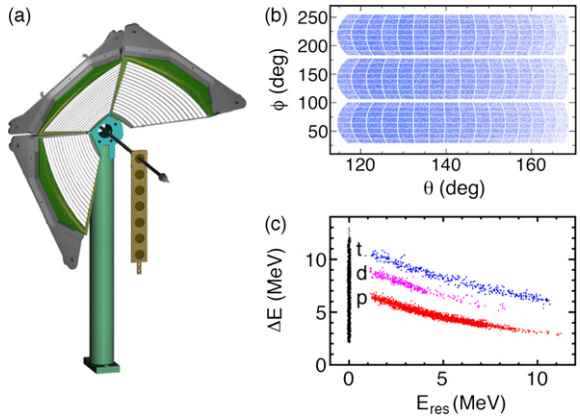

Fig. 1. (a) Arrangement of the basic detector array of four DSSDs, with the beam (arrow) and target ladder. The central detector element contains two DSSDs back to back. (b) The array covers 50° in scattering angle θ and 210° in azimuthal angle ϕ. Pixel separation in each detector is exaggerated for clarity. (c) Typical energy loss ΔE vs. residual energy E_{res} recorded by the detector telescope, for protons (red), deuterons (magenta), and tritons (blue). Particles (black) that deposit all their energy in the first (ΔE) detector cannot be identified individually, but are identified through the kinematic reconstruction of the breakup event. (For interpretation of the references to colour in this figure legend, the reader is referred to the web version of this Letter.)

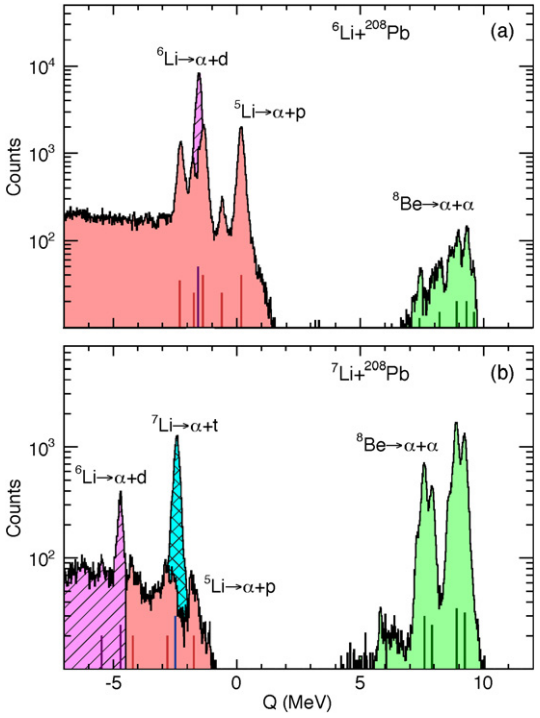

Fig. 2. Measured Q-spectra for the indicated reactions at $E_{beam} = 29.0$ MeV. Identified breakup modes, consistent with the calculated Q-values (vertical bars), are indicated for $\alpha + p$ (red), $\alpha + d$ (magenta), $\alpha + t$ (blue), and $\alpha + \alpha$ (green) pairs. (a) The vertical red bars indicate the Q-values for breakup following the population of the four lowest energy states in ^{209}Pb, the green bars the four lowest energy states in ^{206}Tl, and the magenta bar the ^{208}Pb ground-state. (b) The magenta bars indicate the lowest two states in ^{209}Pb, the red bars the first three states in ^{210}Pb, whilst the blue bar corresponds to the ground state of ^{208}Pb. The green bars indicate the four lowest energy states of ^{207}Tl. (For interpretation of the references to colour in this figure legend, the reader is referred to the web version of this Letter.)

fragments over a wide angular range. In this work, coincidence measurements were made of breakup fragments from reactions of ^{6,7}Li $+^{208}$ Pb at beam energies (E_{beam}) of 24.0, 26.5, and 29.0 MeV. These are all *below* the fusion barrier energies, expected to be $\gtrsim$30 MeV [15]. By measuring below barrier, absorption of breakup fragments was suppressed, eliminating many uncertainties [22]. Furthermore, it allows investigation of the low impact parameter trajectories expected to result in fusion at above-barrier energies.

Beams of ^{6,7}Li from the 14UD electrostatic accelerator at the Australian National University were incident on a 98.7% enriched ^{208}PbS target, 170 μg cm^{-2} in thickness, evaporated onto a 15 μg cm^{-2} carbon backing. The detector system [23] consisted of large area double-sided silicon strip detectors (DSSDs), 400 μm in thickness, with 128 pixels each, in a lamp-shade configuration with apex angle 45°, illustrated in Fig. 1(a). They covered scattering angles from 117° to 167°, and 210° in azimuthal angle. Placing the detector at backward angles minimised the background from elastically scattered beam particles and from the forward focused products from reactions with low Z impurities such as C, O, and S. A measurement with a C target showed that the kinematical reconstruction method (discussed later) eliminates interference with the reactions of interest.

To obtain continuous reconstructed angle spectra, as shown in Fig. 1(b), events were randomised within each pixel. The central detector had a second identical detector placed 5 mm behind to create a detector telescope. This allowed the identification of isotopes of hydrogen (shown in Fig. 1(c)), as well as determination of the energy of the longest range protons. Only data where two DSSD arcs fired were recorded, to minimise the data collection rate. The energy calibration utilised scattered Li and proton beams, and decay α-particles. The energy loss in 0.7 μm PET foils in front of the detectors (to stop low energy electrons), and in the dead layer of the detectors was accounted for event-by-event. The kinetic energy, scattering angle and azimuthal angle (E_i, θ_i, ϕ_i) were determined for each breakup fragment. From this information, breakup events could be characterised as described below.

The energetically favoured breakup modes of Li involve the production of only two charged fragments, which we detected. The energy of the recoiling target-like nucleus E_{rec} was determined, assuming three body kinematics, through conservation of momentum [23]. From the measured kinetic energies E_1 and E_2 of the two breakup fragments and the laboratory kinetic energy of the incident projectile E_{lab} (derived from E_{beam} after correcting for energy lost in traversing the target), the energy change (Q-value) in the reaction was then determined:

$$Q = E_1 + E_2 + E_{rec} - E_{lab}. \quad (1)$$

The measured Q spectra for ^{6,7}Li reactions on ^{208}Pb at $E_{beam} =$ 29.0 MeV are shown in Fig. 2. The spectra at other (lower) energies show similar features, but with reduced yields. At all the measured energies, almost all the yield is in sharp peaks, showing that the breakup is indeed almost exclusively binary, with breakup modes of $\alpha + \alpha$, $\alpha + t$, $\alpha + d$, and $\alpha + p$ identified using the detector telescope. The *expected* Q-values for each binary breakup process, calculated from the masses of all the products, are consistent with the measurements, and indicated for each breakup mode by vertical bars from the axis.

For ^{6}Li (Fig. 2(a)), the most intense peak, at all bombarding energies, corresponds to breakup of excited states of the projectile into its cluster constituents ($\alpha + d$), as might be expected. However, there are five peaks in the spectrum correspond to breakup into $\alpha + p$, triggered by stripping of a neutron from the projectile, forming the unbound ^{5}Li, and ^{209}Pb in its five lowest energy states. After detector efficiency correction (Fig. 4(e)), breakup following transfer is more probable than direct breakup into $\alpha + d$. The small $\alpha + \alpha$ yield results from pick-up of a neutron and a proton, forming ^{8}Be which subsequently decays into two α-particles. Events with $Q < -3$ MeV mainly result from incomplete energy

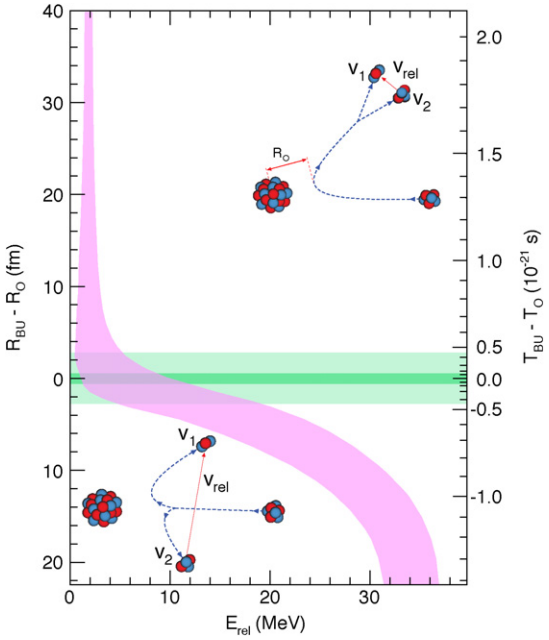

Fig. 3. The curved pink band shows the classically calculated spread of E_{rel} versus the nuclear separation (left axis) or time (right axis) at which breakup occurs, relative to the point of closest approach (R_0, T_0), for ^{8}Be in the field of a ^{208}Pb nucleus. The spread in E_{rel} arises from the different impact parameters and projectile orientations. Breakup prior to reflection, $(T_{BU} - T_0) < 0$, sketched in the lower inset, results in higher E_{rel} values than breakup after reflection $(T_{BU} - T_0) > 0$ (upper inset). The horizontal bands show the 50% (dark) and 95% (light) probability regions for proton pick-up by ^{7}Li to form ^{8}Be (see text). (For interpretation of the references to colour in this figure legend, the reader is referred to the web version of this Letter.)

deposition, due to a proton or deuteron punching through the two single element DSSDs.

For ^{7}Li (Fig. 2(b)), breakup into $\alpha + t$ is prominent, as expected. However, production of ^{8}Be (through pick-up of a proton), with subsequent breakup into two α-particles, is much more likely. The Q spectrum shows that the heavy product ^{207}Tl is populated mainly in its four lowest energy states. The other breakup modes, $\alpha + d$ and $\alpha + p$, are triggered by stripping of neutron(s) from the projectile, forming ^{6}Li and ^{5}Li respectively.

3. Breakup time-scale

Identification of the reaction processes leading to breakup is not sufficient to understand the interplay between breakup and suppression of fusion [15]. It is critical to also know whether the breakup occurs before or after the projectile reaches its point of closest approach to the target nucleus. For example, although formation of ^{8}Be through proton transfer can only occur close to the target nucleus, its ground-state lifetime [6] is long: $\sim 10^{-16}$ s. It will thus decay into two α-particles after receding many thousands of nuclear diameters, and thus its decay can have no effect on fusion. Excited states of ^{8}Be have much shorter lifetimes [6], but the Q-value spectra give no clue to their population. Unlike excited states of the heavy reaction partner, which typically decay by emission of γ-rays in $> 10^{-12}$ s, breakup of the light partner must occur before γ-ray emission, thus the energy of the excited states appears in the fragment kinetic energies, and so cannot be determined from the Q-spectra. However, this crucial information on excited states and time-scales can be extracted from a second derived variable, as discussed next.

Considering these nuclear collisions classically, we can picture the Coulomb field associated with the target nucleus as a spherical mirror. Breakup into two charged fragments after passing the point of closest approach (i.e. after reflection) will give very different fragment trajectories compared to breakup before, as sketched in the top and bottom insets of Fig. 3 respectively. These different outcomes can be best characterised by the relative energy between the fragments, determined from their relative velocity, and expressed in terms of the measured energies E_i and deduced masses m_i, and the measured angular separation θ_{12} of the fragments:

$$E_{rel} = \frac{m_2 E_1 + m_1 E_2 - 2\sqrt{m_1 E_1 m_2 E_2}\cos\theta_{12}}{m_1 + m_2}. \tag{2}$$

The quantitative dependence of E_{rel} on the internuclear separation at breakup can be determined classically, using a three-body three-dimensional model [24,25] developed to relate breakup and fusion. As an example, E_{rel} distributions have been calculated for breakup of ^{8}Be (formed following proton transfer to ^{7}Li), from a nominal 2 MeV excitation energy. Fig. 3 shows the dependence of E_{rel} on the nuclear separation R_{BU} (or time T_{BU}) at which breakup occurs, relative to the point of closest approach without breakup R_0 (T_0). The spread in E_{rel}, shown by the curved pink band, arises from random orientations at breakup, and the range of impact parameters considered (corresponding to angular momenta up to $14\hbar$).

The strong variation of the calculated E_{rel} around R_0 (T_0) indicates that breakup close to R_0 will be characterised by a broad E_{rel} distribution (the energy-time uncertainty relation will further broaden E_{rel}). On the other hand, the asymptote towards 2 MeV after R_0 shows that breakup when moving away from the target will be characterised by a peak at lower E_{rel}. Thus the measured E_{rel} spectra are expected to show two components. The first consists of peaks at low E_{rel} values, centred at $E_{rel} = E^* + Q_{BU}$, where E^* is the excitation energy of the state from which breakup occurs and Q_{BU} is the breakup Q-value. These peaks are associated with breakup on the outgoing trajectory, and thus cannot suppress fusion. The second component consists of events extending to high E_{rel}, which are associated with breakup close to the target nucleus. It is these breakup events that must be responsible for the suppression of fusion observed at above-barrier energies [15,16,18].

Because of the possible population of relatively long-lived (resonant) states in the projectile-like nuclei, it is crucial to make a clear distinction between the locations (and times) of the processes triggering breakup, and those of the breakup itself. Theoretically [24] and experimentally [19,23] it has been shown that below the barrier, the probability of breakup is well described by an exponential dependence on nuclear separation. For each of the mechanisms observed to trigger breakup, we have determined the exponential slope [19,23] from our measurements of the probabilities as a function of beam energy. The horizontal bands in Fig. 3 show the corresponding 50% (dark shading) and 95% (light shading) probabilities for proton pickup by ^{7}Li, which serves as a trigger for breakup. As expected, the probability is strongly peaked around the distance of closest approach R_0, and thus around T_0. For fusion to be suppressed, breakup of ^{8}Be into two fragments must occur before the projectile passes R_0, and starts receding from the target nucleus. From the mapping between radius and time, we can thus conclude that breakup time-scales of $\sim 10^{-22}$ s are required for prompt breakup which at higher beam energies will suppress complete fusion.

The relationship described between the E_{rel} spectrum and the times of breakup shows that the experimental E_{rel} spectra indeed give the critical breakup time-scale information. Thus in conjunction with the Q-spectra, the relative importance of each mechanism leading to prompt breakup can be determined.

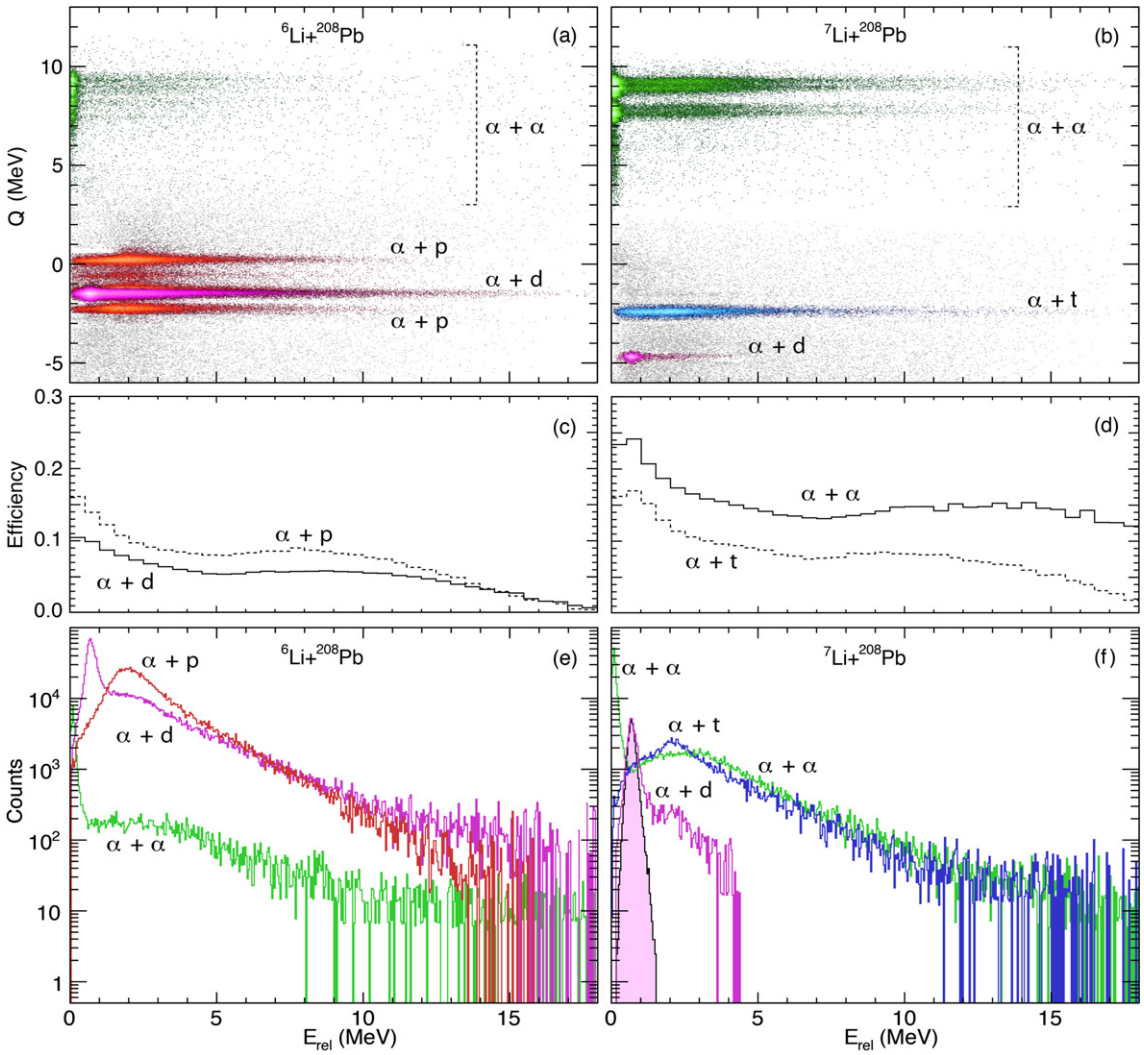

Fig. 4. (a), (b) Two-dimensional Q–E_{rel} correlations for all breakup coincidence pairs, $\alpha + p$, $\alpha + d$, $\alpha + t$, and $\alpha + \alpha$, observed in collisions of ^{6,7}Li with ^{208}Pb at $E_{beam} =$ 29.0 MeV. The reconstructed E_{rel} gives information on the excitation energies of the projectile-like nuclei which cannot be extracted from the Q spectra alone. The intensity of counts is indicated by the brightness of the shading. (c), (d) The detector efficiency response for each breakup process. (e), (f) Efficiency corrected E_{rel} spectra for the major breakup partitions. The peak at 0.7 MeV for $\alpha + d$ pairs corresponds to decay of the first excited state in ^{6}Li. It is too slow to influence fusion. The dominant breakup mode which can suppress complete fusion of ^{6}Li is n-stripping leading to breakup of ^{5}Li into $\alpha + p$. The low energy peak at 92 keV, from $\alpha + \alpha$ pairs, results from the ground state decay of ^{8}Be. The yield at high E_{rel} for breakup into $\alpha + \alpha$ shows that breakup from excited ^{8}Be is dominant in reactions of ^{7}Li. The shaded peak in (f) is from a simulation showing the instrumental resolution in E_{rel}, matching the experimental peak very well.

4. Interpretation of measured E_{rel}

The experimental E_{rel} for each pair of coincident breakup fragments was determined using Eq. (2). The measured E_{rel} vs. Q spectra for ^{6}Li and ^{7}Li at $E_{beam} = 29.0$ MeV are shown in Fig. 4(a), (b). These spectra give the first *complete* picture of breakup in the reactions of these nuclei, since for each breakup mode – identified by its Q-value – determination of E_{rel} allows separation between prompt and delayed breakup, as described below.

The features of the experimental E_{rel} distributions follow qualitatively the expectations from the classical model discussed in Section 3 (and sketched in Fig. 3), namely narrow peaks at low E_{rel} and broad components extending to high E_{rel}. To obtain quantitative probabilities, the E_{rel} spectra have been corrected for detection efficiency through an iterative process. First, the experimentally measured breakup yields as a function of beam energy for each breakup mode were converted to breakup probability as a function of distance of closest approach. This breakup function, and excitation energies at breakup, were then fed into a classical breakup trajectory calculation [24,25] to predict the breakup fragments angular distributions, E_{rel} spectra, and detection efficiencies. The efficiency-corrected breakup function was then generated and used again until convergence occurred. The excitation energies at breakup were adjusted so that the simulated detected events had the same E_{rel} and θ_{12} spectra as measured. The resulting efficiencies of the detector array for the major breakup modes are shown in Fig. 4(c), (d), and the efficiency corrected E_{rel} spectra are in Fig. 4(e), (f).

First the peaks at low E_{rel} are discussed. For both the ^{6}Li and ^{7}Li reactions, the E_{rel} spectra for the $\alpha + \alpha$ breakup mode show a sharp peak at 92 keV corresponding to the slow ^{8}Be ground-state decay. This comprises ∼half of all the $\alpha + \alpha$ yield. For breakup into $\alpha + d$, the peak at 0.7 MeV corresponds to the decay of the first excited state of ^{6}Li, with a relatively long lifetime of 2.7×10^{-20} s. It is populated by direct excitation of ^{6}Li (Fig. 4(e)) or through n-transfer in the ^{7}Li reaction (Fig. 4(f)). The shaded peak in Fig. 4(f) is a simulated E_{rel} spectrum confirming that the

observed width of the 0.7 MeV peak is an effect of instrument resolution arising largely from the pixel size of the DSSDs.

Considering now breakup with higher E_{rel}, for the ^{6}Li reaction breakup into $\alpha + p$ is very significant. It arises from breakup following neutron transfer and makes the largest contribution to prompt breakup in the reaction with ^{6}Li. The remainder is prompt $\alpha + d$ breakup. For the ^{7}Li reaction, breakup into $\alpha + t$ is prominent, with a wide E_{rel} distribution, indicating essentially all prompt breakup. The largest contribution to prompt breakup for ^{7}Li, however, is from prompt breakup of ^{8}Be, i.e. $\alpha + \alpha$ breakup with higher E_{rel}.

Thus for both the ^{6}Li and ^{7}Li reactions, prompt breakup following transfer is more likely than prompt direct breakup into the projectile cluster constituents. The short time-scale of prompt breakup ($\sim 10^{-22}$ s), which gives rise to high E_{rel} components, can only be quantitatively interpreted by quantal reaction models [21,26,27]. This will be a major challenge for the quantum theory of low energy nuclear reactions, requiring new technical developments to allow calculation of relative energy spectra outside the initial mass-partition.

5. Conclusion

These measurements give a complete picture of breakup in reactions of the weakly-bound stable nuclei ^{6,7}Li. Their prompt breakup is found to be triggered by different processes: predominantly *n-stripping* for ^{6}Li, and *p-pickup* for ^{7}Li. The relative energy (E_{rel}) of the two breakup fragments provides information on breakup timescales, and allows prompt breakup modes to be identified. The extreme sensitivity of E_{rel} to the conditions near the point of closest approach of the two nuclei may allow investigation of dynamical modification of nuclear properties [28] – are the properties of excited states of the projectile-like nucleus changed by the close proximity of a heavy nucleus like ^{208}Pb? The demonstration that the reaction dynamics and outcomes can be significantly determined not only by the properties of the two colliding nuclei, but by the ground-state and excited state properties of their neighbours, is a key insight for understanding and predicting reactions of weakly-bound nuclei near the limits of nuclear existence. Furthermore, the results suggest that in sub-barrier collisions of ^{6,7}Li with all but the lightest nuclei, the most likely nuclear reactions will lead to breakup of the projectile-like nucleus, forming elements lighter than Li. This needs to be tested experimentally for reactions with much lighter nuclei, and possible implications for Li abundances in cosmological processes [29,30] investigated. Finally, with further calibration measurements to allow extraction of absolute cross sections from these results, below-barrier cross sections for all significant transfer channels will be available. These will define the coupling strengths for the transfer channels, allowing for the first time reliable coupled-channels calculations and revealing the effects of these transfer couplings on the fusion barrier distributions [31]. This promises to solve quantitatively the puzzling behaviour of ^{6,7}Li in near-barrier nuclear reactions, which has long been a challenge.

References

[1] E. Rutherford, J. Chadwick, Phil. Mag. 42 (1921) 809.
[2] W. von Oertzen, M. Freer, Y. Kanada-En'yo, Phys. Rep. 432 (2006) 43.
[3] F. Hoyle, Astrophys. J. Suppl. Ser. 1 (1954) 121.
[4] E.M. Burbidge, G.R. Burbidge, W. Fowler, F. Hoyle, Rev. Mod. Phys. 29 (1957) 547.
[5] D.R. Tilley, C.M. Cheves, J.L. Godwin, G.M. Hale, H.M. Hofmann, J.H. Kelley, C.G. Sheu, H.R. Weller, Nucl. Phys. A 708 (2002) 3.
[6] D.R. Tilley, J.H. Kelley, J.L. Godwin, D.J. Millener, J.E. Purcell, C.G. Sheu, H.R. Weller, Nucl. Phys. A 745 (2004) 155.
[7] H. Freiesleben, H.C. Britt, J. Birkelund, J.R. Huizenga, Phys. Rev. C 10 (1974) 245.
[8] G.R. Kelly, N.J. Davis, R.P. Ward, B.R. Fulton, G. Tungate, N. Keeley, K. Rusek, Phys. Rev. C 63 (2000) 024601.
[9] R. Ost, K. Bethge, H. Gemmeke, L. Lassen, D. Scholz, Z. Phys. 266 (1974) 369.
[10] J.L. Québert, B. Frois, L. Marquez, G. Sousbie, Phys. Rev. Lett. 32 (1974) 1136.
[11] D. Scholz, H. Gemmeke, L. Lassen, R. Ost, K. Bethge, Nucl. Phys. A 288 (1977) 351.
[12] C. Signorini, A. Edifizi, M. Mazzocco, M. Lunardon, D. Fabris, A. Vitturi, P. Scopel, F. Soramel, L. Stroe, G. Prete, et al., Phys. Rev. C 67 (2003) 044607.
[13] A. Shrivastava, A. Navin, N. Keeley, K. Mahata, K. Ramachandran, V. Nanal, V.V. Parkar, A. Chatterjee, S. Kailas, Phys. Lett. B 633 (2006) 463.
[14] M. Dasgupta, D.J. Hinde, R.D. Butt, R.M. Anjos, A.C. Berriman, N. Carlin, P.R.S. Gomes, C.R. Morton, J.O. Newton, A.S. de Toledo, et al., Phys. Rev. Lett. 82 (1999) 1395.
[15] M. Dasgupta, P. Gomes, D.J. Hinde, S.B. Moraes, R.M. Anjos, A. Berriman, R.D. Butt, N. Carlin, J. Lubian, C.R. Morton, et al., Phys. Rev. C 70 (2004) 024606.
[16] M. Dasgupta, D.J. Hinde, K. Hagino, S.B. Moraes, P.R.S. Gomes, R.M. Anjos, R.D. Butt, A. Berriman, N. Carlin, C.R. Morton, et al., Phys. Rev. C 66 (2002) 041602(R).
[17] C. Signorini, Z.H. Liu, Z.C. Li, K.E.G. Löbner, L. Müller, M. Ruan, K. Rudolph, F. Soramel, C. Zotti, A. Andrighetto, et al., Eur. Phys. J. A 5 (1999) 7.
[18] Y.W. Wu, Z.H. Liu, C.J. Lin, H.Q. Zhang, M. Ruan, F. Yang, Z.C. Li, Phys. Rev. C 68 (2003) 044605.
[19] D.J. Hinde, M. Dasgupta, B.R. Fulton, C.R. Morton, R.J. Wooliscroft, A.C. Berriman, K. Hagino, Phys. Rev. Lett. 89 (2002) 272701.
[20] L.F. Canto, P.R.S. Gomes, R. Donangelo, M.S. Hussien, Phys. Rep. 424 (2006) 1.
[21] N. Keeley, R. Raabe, N. Alamanos, J.L. Sida, Prog. Part. Nucl. Phys. 59 (2007) 579.
[22] F.A. Souza, C. Beck, N. Carlin, N. Keeley, R.L. Neto, M.M. de Moura, M.G. Munhoz, M.G.D. Santo, A.A.P. Suaide, E.M. Szanto, et al., Nucl. Phys. A 821 (2009) 36.
[23] R. Rafiei, R. du Rietz, D.H. Luong, M. Dasgupta, D.J. Hinde, M. Evers, A. Diaz-Torres, Phys. Rev. C 81 (2010) 024601.
[24] A. Diaz-Torres, D.J. Hinde, J.A. Tostevin, M. Dasgupta, L.R. Gasques, Phys. Rev. Lett. 98 (2007) 152701.
[25] A. Diaz-Torres, arXiv:0712.2275, 2007.
[26] Y. Sakuragi, M. Yahiro, M. Kamimura, Prog. Theor. Phys. Suppl. 89 (1986) 136.
[27] I.J. Thompson, Comput. Phys. Rep. 7 (1988) 167.
[28] A.B. McIntosh, S. Hudan, C.J. Metelko, R.T. de Souza, R.J. Charity, L.G. Sobotka, W.G. Lynch, M.B. Tsang, Phys. Rev. Lett. 99 (2007) 132701.
[29] M. Spite, F. Spite, Nature 297 (1982) 483.
[30] H. Utsunomiya, Y. Tokimoto, H. Mabuchi, K. Osada, T. Yamagata, M. Ohta, Y. Aoki, K. Hirota, K. Ieki, K. Iwata, et al., Phys. Lett. B 416 (1998) 43.
[31] M. Dasgupta, D.J. Hinde, N. Rowley, A.M. Stefanini, Annu. Rev. Nucl. Part. Sci. 48 (1998) 401.